Role of Pitx1 Upstream of Tbx4 in Specification of Hindlimb Identity

Malcolm Logan and Clifford J. Tabin*

In spite of recent breakthroughs in understanding limb patterning, the genetic factors determining the differences between the forelimb and the hindlimb have not been understood. The genes *Pitx1* and *Tbx4* encode transcription factors that are expressed throughout the developing hindlimb but not forelimb buds. Misexpression of *Pitx1* in the chick wing bud induced distal expression of *Tbx4*, as well as *HoxC10* and *HoxC11*, which are normally restricted to hindlimb expression domains. Wing buds in which *Pitx1* was misexpressed developed into limbs with some morphological characteristics of hindlimbs: the flexure was altered to that normally observed in legs, the digits were more toe-like in their relative size and shape, and the muscle pattern was transformed to that of a leg.

In most respects the genetic systems controlling limb development act equivalently in the chick forelimb (wing) and hindlimb (leg) buds. However, as is true for the human arm and leg, the chick wing and leg have very different morphologies. Several genes have been described that are expressed in a manner consistent with their playing a role in limb-type specification. *Pitx1*, an *Otx*-related paired-type homeobox transcription factor, is expressed in the developing hindlimb bud but not forelimb bud (*1–3*). Two T-box family transcription factors *Tbx5* and *Tbx4* are expressed, respectively, in the forelimb bud and hindlimb bud in the mouse (*4*) and newt (*5*). Moreover, the correlation between the expression of these genes and limb identity is maintained after various surgical manipulations in the chick (*6–10*). We focused our initial functional analysis on *Pitx1* because it is expressed before the *Tbx* genes in prelimb stage chick embryos (*6*) and might therefore act upstream of them in limb-type specification.

We injected a retroviral vector carrying *Pitx1* into the wing field of stage 9-10 embryos and examined the expression of various limb-type–specific markers between stages 22 and 27 (*11*). We observed ectopic induction of *Tbx4* in forelimbs where *Pitx1* was successfully misexpressed ($n = 13$). This ectopic expression was largely limited to the distal mesenchyme at stage 22 and its subsequent derivatives in later limb buds (Fig. 1). Although virus is introduced before limb formation, there is a delay of 16 to 18 hours after infection before the transgene is actively expressed. Thus, induction of *Tbx4* in response to *Pitx1* expression may be restricted to the undifferentiated cells still in the distal progress zone when Pitx1 protein is first ectopically produced. After infection with *Pitx1*, ectopic *Tbx4* induction was also seen in the interlimb flank mesoderm (*12*), which is capable of giving rise to ectopic limbs after application of fibroblast growth factors (*13–16*). However, we never saw *Tbx4* induction in infected limb bud ectoderm and there was no *Tbx4* induction in *Pitx1*-infected somites or paraxial mesoderm.

Because *Tbx4* and *Tbx5* are normally found in mutually exclusive limb territories, it was possible that *Pitx1* might also act to repress the forelimb-specific gene *Tbx5*, either directly or through mutual transcriptional antagonism between *Tbx4* and *Tbx5*. We examined *Tbx5* expression in wing buds after *Pitx1* misexpression but never observed any change in *Tbx5* expression, even in domains where *Tbx4* is up-regulated (Fig. 1; $n = 22$). Another possible regulatory pathway could lead to autoregulation of *Pitx1*; however, we found no evidence of endogenous *Pitx1* induction in infected wing buds, including its absence in the distal domain where *Tbx4* was ectopically induced [(*12*); $n = 13$]. Thus in a linear pathway, *Pitx1* induces expression of the second hindlimb-specific gene *Tbx4*, whereas the forelimb-specific gene *Tbx5* is under independent control. This induction is specific in that *Tbx4* was never induced in limb buds infected with the closely related gene *Pitx2* [(*12*, *17*); $n = 9$].

A number of other genes show limb-type–specific expression patterns, for example *HoxC10* and *HoxC11* in the hindlimb buds (*18*). These genes are unlikely to play a primary role in establishing limb identity, as they are expressed in limited subdomains of the hindlimb bud and are expressed relatively late during limb development. Nevertheless, they are excellent candidates for genes involved in mediating aspects of hindlimb-specific morphogenesis. We found that both *HoxC10* and *HoxC11* were induced ectopically in infected wing buds (Fig. 1; *HoxC10*, $n = 15$; *HoxC11*, $n = 7$). Only the distal and posterior expression of their respective leg domains were recapitulated in *Pitx1*-infected wings. Thus, at a molecular level, *Pitx1* induces hindlimb-specific changes when misexpressed in wing buds.

To examine the morphological consequences of *Pitx1* misexpression, we infected the wing territories of stage 8-9 chick embryos with the *Pitx1* virus, and the embryos were allowed to develop until stages 35 to 37. Immediately obvious, at a gross morphological level, was a change in the overall flexure of the limb (Fig. 2, B and D). The autopod (hand and digits) of the normal chick wing is posteriorly flexed relative to the zeugopod (lower arm). The digits remain in the anteri-

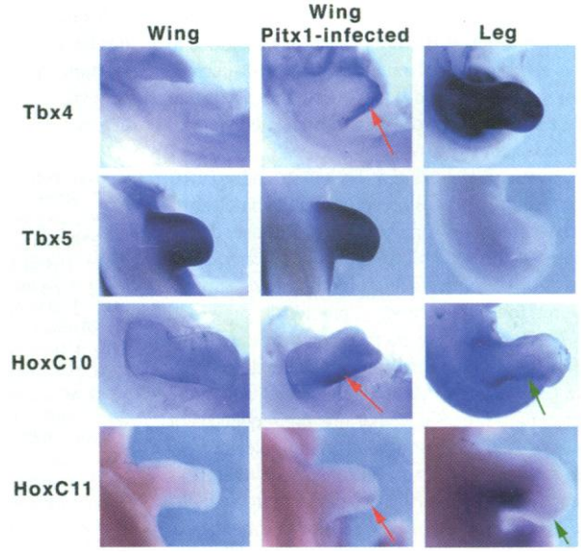

Fig. 1. Ectopic induction of hindlimb-specific genes after ectopic expression of *Pitx1*. Whole-mount in situ hybridization was carried out with probes for *Tbx4*, *Tbx5*, *HoxC10*, and *HoxC11*, as indicated at the left of each row. The contralateral, uninfected wing is shown in the left column (these images have been reversed in their horizontal plane for easier comparison), the normal expression in the leg is shown in the right column, and the *Pitx1*-infected wings are shown in the central column. The examples shown for each gene are from the same embryo: *Tbx4* and *HoxC11*, stage 25; *Tbx5*, stage 24; and *HoxC10*, stage 26. Red arrows point to domains of ectopic *Tbx4*, *HoxC10*, and *HoxC11* in *Pitx1*-infected limbs. Green arrows point to the endogenous posterior domain of *HoxC10* and the endogenous distal, posterior domain of *HoxC11* in normal limbs, which are recapitulated in the *Pitx1*-infected limbs.

Department of Genetics, Harvard Medical School, 200 Longwood Avenue, Boston, MA 02115, USA.

*To whom correspondence should be addressed. E-mail: tabin@rascal.med.harvard.edu

or-posterior plane in which they formed (Fig. 2A). In contrast, in the normal hindlimb there is no equivalent posterior flexure at the ankle; the distal elements of the leg are maintained in a straight orientation. In addition, the autopod is rotated 90° such that the digits are in a horizontal position for walking, with the former anteriormost digit becoming medial and the more posterior digits becoming sequentially more lateral in position (Fig. 2C). In the chick, this rotation begins around stage 30 and is complete around stage 34 (*19*). The *Pitx1*-infected wings were often held in a leglike position in both respects, showing no posterior flexure at the wrist and having the digits rotated 90° (Fig. 2, B and D). None of the examples in which *Pitx1* was successfully misexpressed had normal posterior flexure at the wrist. The rotation of the digits 90° was a more variable phenotype. Although all the examples showed at least some degree of rotation, only a minority were rotated fully 90° (n = 4/11). There are also distinctions between the ectodermal derivatives in the wing and leg. The wing uniquely has a flap of skin, the patagium, extending between the flexed upper and lower arm (Fig. 2A). In all *Pitx1*-infected limbs, the patagium was absent or severely reduced in size (Fig. 2, B and D). Because after infection the flexure of the upper limb is unchanged, the absence of the patagium is not a simple consequence of the angle of the limb, but a direct result of the patterning alterations due to *Pitx1*.

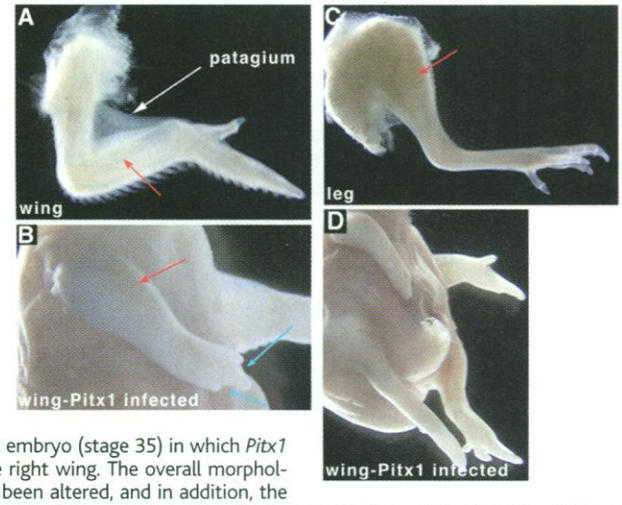

Fig. 2. Gross morphology of normal and *Pitx1*-infected limbs. (**A**) Normal wing, stage 36. (**B**) *Pitx1*-infected wing, stage 35. In the *Pitx1*-infected wing, the normal flexure of the wing has changed, no patagium has formed, and the ectoderm is smooth, with no evidence of formation of nascent featherbuds. The blue arrows indicate the areas of interdigital cell death at the distal extreme of the limb, as normally occurs in the leg. (**C**) Normal leg, stage 36. Red arrows are discussed in the text. (**D**) An example of a different embryo (stage 35) in which *Pitx1* has been misexpressed in the right wing. The overall morphology of the infected wing has been altered, and in addition, the digits have rotated 90° relative to their normal position (compare with the uninfected, left wing) and are now aligned similarly to the digits of the leg.

Another ectodermal difference between fore- and hindlimbs in the chicken is that the wing forms feathers whereas the distal leg forms scales. Wings in which *Pitx1* was misexpressed always showed at least some loss of normal featherbud formation (Fig. 2) (*12*), although the degree of loss was variable. Affected areas were always distally restricted and were correlated with regions of the wing bud in which the normal morphology had been most obviously grossly affected. Infected wings, however, did not develop scales but rather remained smooth on their surface. Although it is not clear why scales did not form, in principle the smooth ectoderm could have resulted as a nonspecific suppression of ectodermal appendage formation when *Pitx1* was ectopically expressed in the ectoderm. However, *Pitx1* never disrupted scale formation when misexpressed in the hindlimb, and importantly, no suppression of featherbud formation was observed after *Pitx1* misexpression in the flank (*12*). This indicates that *Pitx1* expression per se is not incompatible with feather formation. Rather, we propose that the loss of feathers in infected wings is a patterning defect due to the misexpression of this hindlimb-specific gene in the wing.

To analyze the changes in skeletal pattern induced by *Pitx1* misexpression, we cleared and stained infected wings with Alcian blue (n = 12) (*20*). In the normal leg, digits II, III, and IV, which form the forward-pointing toes, are of approximately equal length, and there is an additional small anterior digit I that ultimately rotates to point toward the back of the foot (Fig. 3C). In infected wings, digits II, III, and IV were similar in size (Fig. 3B). In some cases there were modified wing digits II, III, and IV, with digit II being notably extended (*12*). In other examples, there was a fourth digit, often formed by bifurcation of wing digit III (Fig. 3D), whereas the anteriormost wing digit II remained short, approximating the normal leg digit I (n = 4/12). Although the number of phalangeal elements in each digit remained unchanged after *Pitx1* misexpression, the shapes of many of the individual bone elements in the digits were more similar to those found in the leg (Fig. 3B). Moreover, at the tips of the these digits, claws formed, which are normally seen only on hindlimbs (Fig. 3B, red arrow; n = 6/12). In addition, an apparent change occurred in the pattern of interdigital cell death. In the normal leg, interdigital cell death results in a separation of each of the digits (Fig. 3C), whereas in the wing, digits III and IV remain together surrounded by soft tissue (Fig. 3A). In infected wings there was at least partial separa-

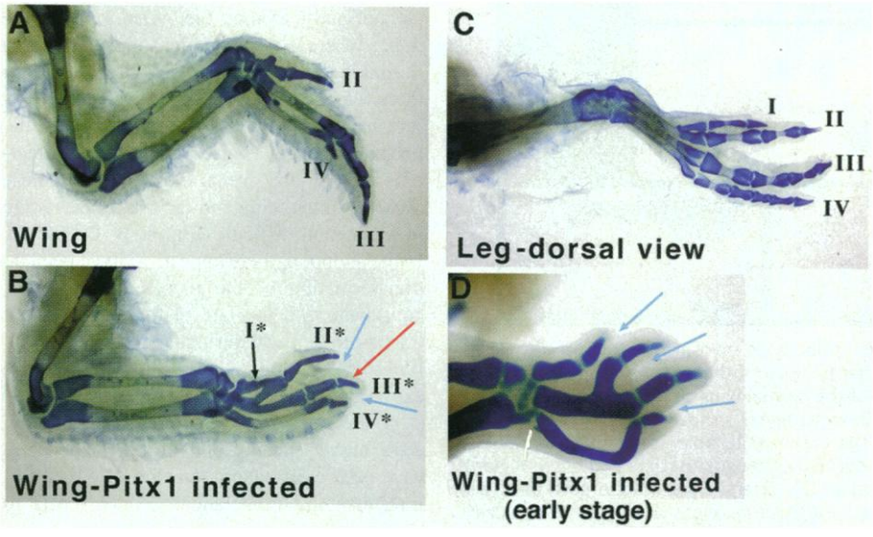

Fig. 3. Alcian blue staining of the skeletal elements of normal and *Pitx1*-infected limbs. (**A**) A normal wing, (**B**) a *Pitx1*-infected wing, and (**C**) a normal leg at stage 38. The digit patterns are indicated with roman numerals, wing II to IV and leg I to IV. The digits in the *Pitx1*-infected wing (distinguished with an asterisk) are more uniform in length and contain some phalangeal elements most similar to those in the foot. A claw on digit III* is indicated by the red arrow. In addition, four digits have formed instead of three. The extra digit often forms by a bifurcation of wing digit III, as can be seen in an infected wing harvested at stage 33 when the cartilage elements are forming (**D**). The blue arrows indicate areas of interdigital cell death around the transformed digits.

tion of the distal ends of digits III and IV (Figs. 2B and 3B) and in some cases the digits separated completely (Fig. 3D). Finally, the change in wrist flexure was also clear in the skeletal preparations. For example, the characteristic downward flexure at the wrist was lost in the *Pitx1*-infected wing and instead the digits pointed straight out in a similar fashion to the digits of the foot at the ankle (Fig. 3B). On the basis of the molecular analysis, it is not surprising that *Pitx1* only induced a partial forelimb-to-hindlimb transformation, because the normal expression of the forelimb-specific gene *Tbx5* is maintained in addition to the ectopic expression of the hindlimb-specific gene *Tbx4*. However, a more complete transformation was observed when the soft tissues were analyzed.

The limb-type–specific patterning of the soft tissues is, at least to some extent, independent of the skeletal patterning, because wing-specific muscles form even in the absence of any skeletal elements (*21*). Because *Pitx1* is expressed throughout the hindlimb mesenchyme, it seemed likely that *Pitx1* might, either directly or indirectly, modulate the patterning of the musculature in addition to the skeleton. Moreover, because the undifferentiated myoblasts migrate into the limb bud after proximal skeletal elements have been specified, it was possible that *Pitx1* infection might be able to alter muscle patterning at a more proximal level than observed for the bones. Indeed, gross morphological examination showed that the soft tissue of the infected zeugopod (level of the radius and ulna) bulged dorsally like the shank of the leg (level of the tibia and fibula) and unlike the morphology of that region of normal wings (Fig. 2, red arrows).

To directly examine the effect of *Pitx1* on muscle patterning, we stained infected and control stage 32-36 limbs with a muscle-specific antibody to myosin (MF20) (*20*). The zeugopod of a normal stage 32 wing contains 6 muscles dorsally and 7 muscles ventrally (Fig. 4, A and B) (*22*), whereas the leg contains 4 muscles dorsally and 12 muscles ventrally (Fig. 4, E and F) (*23, 24*). Importantly, each of these muscles is uniquely defined by characteristic shape, position, pattern of fiber orientation, origin, and insertion. Together, these characteristics allow each muscle in the wing and leg to be unambiguously distinguished. In *Pitx1*-infected limbs the overall muscle pattern underwent a dramatic transformation (n = 9/11). This was particularly apparent on the dorsal side (Fig. 4, C, D, and H). The extensor digitorum longus (EDL) (Fig. 4, E and F, in detail I) is uniquely identifiable by its central dorsal position, narrow fusiform shape, and characteristic bipennate fiber pattern (fibers in the anterior and posterior of the muscle are arranged at opposing angles; Fig. 4G). Moreover, this muscle is attached to a large central tendon that extends to each of the hindlimb digits (it is the muscle controlling release of the digits from a flexed, perching position). There is no equivalent muscle, either in morphology or in tendon attachment, in the wing. In infected wings there was a clearly identifiable EDL (in 2/11 the transformation to an EDL was complete in all respects) (Fig. 4, D and H). A similar muscle transformation was seen in the formation of a leg-specific fibularis brevis (FB) in infected limbs, which is distinguished by its distal lateral position, short rectangular shape and unipennate fiber pattern (Fig. 4, C and D) (*25*). Two other muscles seen in *Pitx1*-infected wings were similar in shape and position to the normal hindlimb tibialis cranialis and fibularis longus (Fig. 4, C and D).

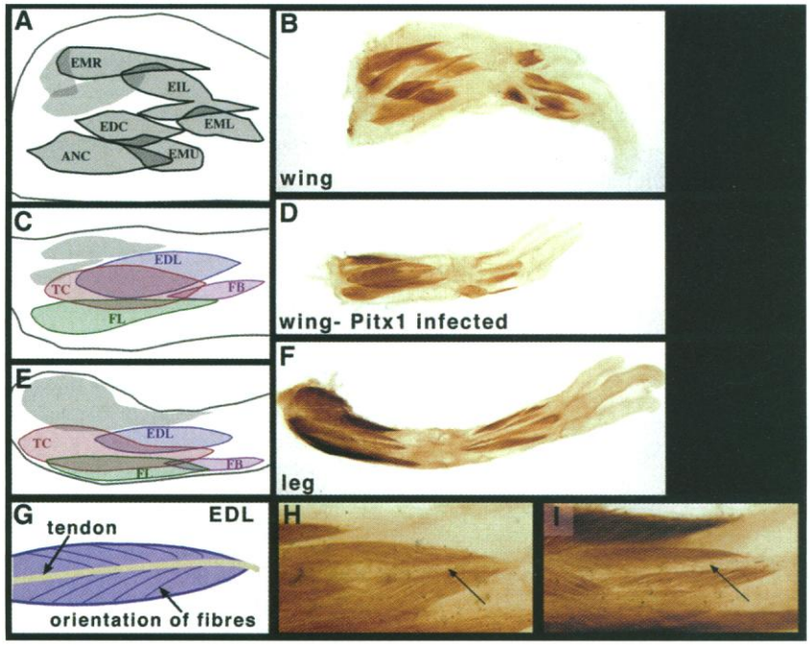

Fig. 4. Whole-mount immunohistochemistry with an antibody to myosin that identifies the limb musculature. Dorsal views are shown. For improved clarity, most of the underlying ventral muscles have been removed. (**A**) A schematic of the muscles of the normal wing zeugopod (radius and ulna region). The entire limb, from stylopod to autopod (elbow to digits) is shown in (**B**). (**C**) A schematic of the muscles in a *Pitx1*-infected wing zeugopod. The entire limb, from stylopod to autopod is shown in (**D**). (**E**) A schematic of the muscles of the normal leg zeugopod (tibia and fibula region). The entire limb from stylopod to autopod is shown in (**F**). Overall, the muscle pattern in the *Pitx1*-infected wing is altered. In particular, a leg extensor digitorum longus (EDL) is present, as well as fibularis brevis (FB), tibialis cranialis (TC), and fibularis longus (FL) [(C) and (D)]. The muscles can be unambiguously identified by shape, origin and insertion, and patterns of fiber orientation. In the normal EDL [shown schematically in (**G**) and in detail in (**I**)], the fibers angle distally and medially to the thick central tendon (arrow), which ultimately splits to control the extension of each digit. A detail of the transformed EDL is shown in (**H**). The muscles shaded in light gray in (C) and (E) have a ventral origin and were not included in the comparison. In the wing schematic in (A), the muscles shaded in gray do not send tendons across the wrist and are not described. EMR, extensor metacarpi radialis; EIL, extensor indicis longus; EDC, extensor digitorum communis; EML, extensor medius longus; ANC, anconeus; EMU, extensor metacarpi ulnaris.

On the ventral side, specific transformation of muscle type was harder to classify. There was, however, an increased number of muscles (*9*), which is more characteristic of the leg (*12*). Moreover, there was a change in the attachment of the flexor digitorum superficialis in the wing. This characteristic muscle normally crosses the wrist joint in the wing, whereas no equivalent muscle crosses the ankle joint in the leg. After *Pitx1* infection there was no extension of any muscle crossing the wrist joint (*12*). In the autopod, the muscle pattern was also altered in the infected wings, but the similar morphology of these muscles in the wing and leg makes definitive identification difficult (Fig. 4, B, D, and F). In the stylopod, there appears to have been no transformation of the muscle pattern (*12*), consistent with the fate of this region being the first to be fixed during development of the limbs and with the lack of affect on gene expression in the proximal wing bud.

The effects of *Pitx1* on muscle organization were highly specific and in detail appear to have been clear pattern transformations; therefore, the muscle alterations do not appear to have been secondary consequences, for example, of changes in the size of the limb bud. Indeed, after *Pitx1* infection the length of the zeugopod in the infected wing and in the contralateral wing were identical (Fig. 4). It should be noted that muscles can affect skeletal development, and therefore the transformation of muscle identity in *Pitx1*-infected wings could

be at least partly responsible for the transformation of skeletal morphology observed. Furthermore, the transformation of muscle and distal tendon attachments could cause the apparent footlike flexure we describe above (Fig. 2). As with the skeletal transformations, the effect of *Pitx1* on muscle pattern is specific to the hindlimb gene *Pitx1* because parallel misexpression of a highly related control gene, *Pitx2*, did not have an effect on soft tissue morphology, in spite of the fact that this gene had a high biological activity in other contexts (*17*). Because comparatively little is known about the molecular basis for muscle patterning, the ability of *Pitx1* to respecify muscle identity will provide a useful tool in this regard, in addition to being evidence for a role of *Pitx1* in the specification of hindlimb patterning.

In summary, we found that *Pitx1* acts upstream of *Tbx4* and regionally expressed *Hox* genes in a pathway that regulates limb-type identity. The correct induction of the forelimb- or hindlimb-specific genes in the respective limb fields must depend on upstream genes that regionalize the rostral-caudal body axis, which is likely ultimately dependent on axial expression of *Hox* genes. Further gain- and loss-of-expression studies with other genes in this pathway will provide additional insight into the mechanism by which the common aspects of limb patterning are modified to produce limb-type–specific morphologies.

References and Notes

1. D. P. Szeto, A. K. Ryan, S. M. O'Connell, M. G. Rosenfeld, *Proc. Natl. Acad. Sci. U.S.A.* **93**, 7706 (1996).
2. T. Lamonerie *et al.*, *Genes Dev.* **10**, 1284 (1996).
3. J. Shang, X. Li, H. Z. Ring, D. A. Clayton, U. Francke, *Genomics* **40**, 108 (1997).
4. J. J. Gibson-Brown *et al.*, *Mech. Dev.* **56**, 93 (1996).
5. H.-G. Simon, *et al.*, *Development* **124**, 1355 (1997).
6. M. Logan, H.-G. Simon, C. Tabin, *ibid.* **125**, 2825 (1998).
7. H. Ohuchi *et al.*, *ibid.*, p. 51.
8. A. Isaac *et al.*, *ibid.*, p. 1867.
9. J. J. Gibson-Brown, S. I. Agulnik, L. M. Silver, V. E. Papaioannou, *ibid.*, p. 2499.
10. C. Lanctot, B. Lamolet, J. Drouin, *ibid.* **124**, 2807 (1997).
11. Fertilized White Leghorn chicken eggs were incubated at 37°C in a humidified incubator and the stage of development was determined according to the guidelines of Hamilton and Hamburger (*19*). We cloned the entire open reading frame of chick *Pitx1* into the RCAS plasmid using conventional methods (*26*). Viral infection was carried out on embryos at stage 10. The presumptive wing and leg territories were targeted as previously described in (*26*), whole-mount in situ hybridizations were carried out essentially as described in [R. D. Riddle, R. L. Johnson, E. Laufer, C. J. Tabin, *Cell* **75**, 1401 (1993)], and 20-μm-cryosection in situ hybridizations were carried out essentially as described in [Z. Z. Bao and C. L. Cepko, *J. Neurosci.* **17(4)**, 1425 (1997)]. Probes for *HoxD9*, *HoxC9*, *HoxC10*, and *HoxC11* are described in (*18*) and those for *Tbx4*, *Tbx5*, and *Pitx1* are described in (*6*). A probe template specific for the 3′ untranslated region (UTR) of *Pitx1* was generated by polymerase chain reaction with a *Pitx1* 3′-UTR forward primer TGACACGAACCACCTCCG, an M13 universal primer as reverse primer, and a full-length library isolate (OT17) as template. Antisense probes were made with T7 RNA polymerase.
12. M. Logan and C. J. Tabin, data not shown.
13. M. J. Cohn, J.-C. Izpisua-Belmonte, H. Abud, J. K. Heath, C. Tickle, *Cell* **80**, 739 (1995).
14. H. Ohuchi *et al.*, *Biochem. Biophys. Res. Commun.* **209**, 809 (1995).
15. P. H. Crossley, G. Minowada, C. A. MacArthur, G. A. Martin, *Cell* **84**, 127 (1996).
16. A. Vogel, C. Rodriguez, J.-C. Izpisua-Belmonte, *Development* **122**, 1737 (1996).
17. M. Logan, S. Pagan-Westphal, D. Smith, L. Paganessi, C. Tabin, *Cell* **94**, 307 (1998).
18. C. E. Nelson *et al.*, *Development* **122**, 1449 (1996).
19. V. Hamburger and H. L. Hamilton, *J. Morphol.* **88**, 49 (1951).
20. The cartilage elements were stained with Alcian blue as previously described (*6*). Whole-mount immunohistochemistry with MF20 antibody to muscle myosin was carried out as described [M. W. Klymkowsky and J. Hanken, Eds., *Whole-Mount Staining of* Xenopus *and Other Vertebrates* (Academic Press, San Diego, 1991)]. Detection was carried out with a horseradish peroxidase–conjugated secondary antibody (Jackson Immunoresearch, West Grove, PA, diluted 1:200).
21. M. F. Lanser and J. F. Fallon, *Anat. Rec.* **217**, 61 (1987).
22. G. B. Shellswell and L. Wolpert, Eds., *The Pattern of Muscle and Tendon Development in the Chick Wing* (Cambridge Univ. Press, Cambridge, 1977).
23. R. A. Wortham, *J. Morphol.* **83**, 105 (1948).
24. M.-P. Pautou, I. Heydayat, M. Kieny, *Arch. Anat. Microsc. Morphol. Exp.* **71**, 193 (1982).
25. G. Kardon, *Development* **125**, 4019 (1998).
26. M. Logan and C. Tabin, *Methods Enzymol.* **14**, 407 (1998).

27. We thank L. Paganessi for technical assistance, G. Kardon for help in analysis of the limb musculature and preparing a schematic of the muscle pattern, D. Smith for assisting in injection experiments, and J. C. Izpisua-Belmonte, M. G. Rosenfeld, J. Drouin, and T. Ogura for communicating results before publication. M.L. was funded by a postdoctoral fellowship from the Human Frontier Science Program Organisation. This work was funded by a grant from the NIH.

19 January 1999; accepted 16 February 1999

Negative Regulation of Wingless Signaling by D-Axin, a *Drosophila* Homolog of Axin

Fumihiko Hamada,[1,2] Yoshinori Tomoyasu,[3] Yoshihiro Takatsu,[3] Makoto Nakamura,[3] Shin-ichi Nagai,[3] Akiko Suzuki,[1] Fumitaka Fujita,[1] Hiroshi Shibuya,[3] Kumao Toyoshima,[4] Naoto Ueno,[3] Tetsu Akiyama[1,5*]

Wnt/Wingless directs many cell fates during development. Wnt/Wingless signaling increases the amount of β-catenin/Armadillo, which in turn activates gene transcription. Here the *Drosophila* protein D-Axin was shown to interact with Armadillo and D-APC. Mutation of *d-axin* resulted in the accumulation of cytoplasmic Armadillo and one of the Wingless target gene products, Distalless. Ectopic expression of *d-axin* inhibited Wingless signaling. Hence, D-Axin negatively regulates Wingless signaling by down-regulating the level of Armadillo. These results establish the importance of the Axin family of proteins in Wnt/Wingless signaling in *Drosophila*.

The Wnt/Wingless (Wg) signal-transduction pathway is involved in cell-cell signaling in many developmental processes (*1*). Wnt/Wg signaling promotes the stabilization of β-catenin/Armadillo (Arm, a *Drosophila* homolog of β-catenin) by negatively regulating the activity of glycogen synthase kinase–3β (GSK-3β). β-Catenin/Arm binds to transcription factors of the LEF/TCF family and thereby modulates expression of Wnt/Wg-responsive genes (*2*). The colorectal tumor-suppressor gene product APC induces down-regulation of β-catenin, and mutation of APC results in the accumulation of the latter (*3*). Mutations that activate β-catenin have also been detected in some tumors with intact APC (*4*). Therefore, regulation of the level of β-catenin is critical for Wnt/Wg signaling during development and tumorigenesis. Here, we show that the *Drosophila* protein D-Axin interacts with Arm and D-APC and is a negative regulator of Wg signaling.

To identify Arm-interacting proteins, we performed a yeast two-hybrid screen of a *Drosophila* embryo cDNA library using the Armadillo repeat domain of Arm as target and identified a protein that we designate D-Axin (*5*). Sequence analysis of the *d-axin* cDNA showed that it encodes a protein of 743 amino acids. A region near its NH_2-

[1]Department of Oncogene Research, Research Institute for Microbial Diseases, Osaka University, 3-1 Yamadaoka, Suita 565-0871, Japan. [2]"Inheritance and Variation," Precursory Research for Embryonic Science and Technology (PRESTO), Japan Science and Technology Corporation (JST), Japan. [3]Division of Morphogenesis, Department of Developmental Biology, National Institute for Basic Biology, Myodaijicho, Okazaki 444-8585, Japan. [4]Osaka Medical Center for Cancer and Cardiovascular Diseases, Nakamichi, Higashinari-ku, Osaka 537-8511, Japan. [5]Department of Molecular and Genetic Information, Institute of Molecular and Cellular Biosciences, University of Tokyo, 1-1-1 Yayoi, Bunkyo-ku, Tokyo 113-0032, Japan.

*To whom correspondence should be addressed. E-mail: akiyama@imcbns.iam.u-tokyo.ac.jp